ELSEVIER

Contents lists available at ScienceDirect

Clinical Biomechanics

journal homepage: www.elsevier.com/locate/clinbiomech





Does spinopelvic alignment affect femoral head cartilage and the proximal femoral physis in slipped capital femoral epiphysis? A finite element analysis

Yogesh Kumaran^{a,b}, Muzammil Mumtaz^a, Carmen Quatman^b, Julie Balch-Samora^c, Sophia Soehnlen^{a,b}, Brett Hoffman^a, Sudharshan Tripathi^a, Norihiro Nishida^d, Vijay K. Goel^{a,*}

- a Engineering Center for Orthopaedic Research (E-CORE), Departments of Bioengineering and Orthopaedic Surgery, University of Toledo, Toledo, OH, United States
- b Ohio State University Wexner Medical Center, Department and Orthopaedics, Columbus, OH, United States
- ^c Nationwide Children's Hospital, Department of Orthopedics, Columbus, OH, United States
- ^d Yamaguchi University Hospital, Department of Orthopaedic Surgery, Ube, Yamaguchi, Japan

ARTICLE INFO

Keywords: Slipped capital femoral epiphysis Spinopelvic parameters Finite element analysis

ABSTRACT

Background: Slipped capital femoral epiphysis is a prevalent pediatric hip disorder. Recent studies suggest the spine's sagittal profile may influence the proximal femoral growth plate's slippage, an aspect not extensively explored. This study utilizes finite element analysis to investigate how various spinopelvic alignments affect shear stress and growth plate slip.

Methods: A finite element model was developed from CT scans of a healthy adult male lumbar spine, pelvis, and femurs. The model was subjected to various sagittal alignments through reorientation. Simulations of two-leg stance, one-leg stance, walking heel strike, ascending stairs heel strike, and descending stairs heel strike were conducted. Parameters measured included hip joint contact area, stress, and maximum growth plate Tresca (shear) stress.

Findings: Posterior pelvic tilt cases indicated larger shear stresses compared to the anterior pelvic tilt variants except in two leg stance. Two leg stance resulted in decreases in the posterior tilted pelvi variants hip contact and growth plate Tresca stress compared to anterior tilted pelvi, however a combination of posterior pelvic tilt and high pelvic incidence indicated larger shear stresses on the growth plate. One leg stance and heal strike resulted in higher shear stress on the growth plate in posterior pelvic tilt variants compared to anterior pelvic tilt, with a combination of posterior pelvic tilt and high pelvic incidence resulting in the largest shear.

Interpretation: Our findings suggest that posterior pelvic tilt and high pelvic incidence may lead to increased shear stress at the growth plate. Activities performed in patients with these alignments may predispose to biomechanical loading that shears the growth plate, potentially leading to slip.

1. Introduction

Slipped capital femoral epiphysis (SCFE) is a multifactorial pathology of the hip commonly affecting children between the ages of 8 and 15 years with an incidence of 0.3–2/100,000 (Loder and Skopelja, 2011). Early identification of high-risk patients for SCFE is crucial for implementing preventive strategies against slippage at the proximal femoral physis and its adverse sequelae (Balch Samora et al., 2018). Obesity, endocrinopathies, and vitamin D deficiency are risk factors that have been implicated in its development (Lehmann et al., 2006; Novais

and Millis, 2012). Biomechanical factors, including acetabular version, repetitive weight-bearing activities, sports, and other physical exertions also contribute to increased shear stresses at the proximal femoral physis, leading to slip (Haider et al., 2022; Zupanc et al., 2008). More recently, studies have suggested that the sagittal profile of the spinopelvic complex is a contributing factor to growth plate shear and slip (Gebhart et al., 2015; Wako et al., 2020).

Sagittal balance refers to the physiologic alignment of the spine which maximizes kinetic efficiency and minimizes mechanical stress. Balance exists when an individual's weight is positioned on a vertical

^{*} Corresponding author at: Departments of Bioengineering and Orthopaedic Surgery, Colleges of Engineering and Medicine, University of Toledo, 2801 West Bancroft Street, MS 303, NI Hall, Room 5046, Toledo, OH 43606, United States of America.

E-mail address: Vijay.Goel@utoledo.edu (V.K. Goel).

axis aligned slightly posterior to the rotational axis of the femoral heads (Roussouly et al., 2006; Schwab et al., 2006). Spinopelvic parameters determine the overall sagittal balance of the spinopelvic complex and include lumbar lordosis (LL), sacral slope (SS), pelvic tilt (PT), and pelvic incidence (PI) (Fig. 1) (Ghobrial et al., 2018; Le Huec et al., 2011; Legaye et al., 1998; Polly et al., 2012).

While the relationship between hip and spine mechanics has been extensively studied in adults, its impact on the SCFE population remains less explored (Lazennec et al., 2007; Lazennec et al., 2011). Controversy exists on whether PI and other spinopelvic parameters contribute to SCFE. A cadaveric study performed by Gebhart et al. identified smaller PI angles in post-SCFE deformity patients compared to normal specimens (Gebhart et al., 2015). On the other hand, a retrospective study performed by Wako et al. determined no relationship between PI and SCFE (Wako et al., 2020). These discrepancies highlight the need for biomechanical analyses to understand the role of load distribution on the femoro-acetabular joint and proximal femoral physis due to variations in sagittal spinopelvic parameters.

To the best of the authors' knowledge, no biomechanical study of SCFE encompasses the complete spinopelvic complex, including the femur, hip joint, pelvis, and spine (Castro-Abril et al., 2015; Fishkin et al., 2006; Paseta et al., 2019; Rhyu et al., 2011; Shah, 2005). We hypothesize that sagittal spinopelvic alignment influences stress distribution on the femoral head and proximal femoral physis. This study utilizes a theoretical finite element (FE) model to investigate the contribution of sagittal spinopelvic parameters on SCFE biomechanics.

2. Methods

2.1. Original FE model creation

A non-linear, ligamentous FE model was developed using computed tomographic (CT) scans of a healthy adult lumbar spine, pelvis, and femur with no abnormalities, deformities, or severe degeneration. The CT scans were reconstructed and segmented using MIMICS software (Materialize Inc., Leuven, Belgium). Mesh was applied to the reconstructed geometry using Meshlab Open-Source Software (Cignoni et al., 2008).

Abaqus 2019 (Dassault Systèmes, Simulia Inc., Providence, RI, USA) was used to assemble the meshed components and perform the subsequent analyses. All geometries were imported and the "tri to tet" feature was used to convert the triangular shell surface mesh into solid tetrahedral mesh (C3D4). In the vertebral bodies, pelvis, and femurs, each part's mesh was sectioned to include a 0.5-1 mm cortical bone shell around a core of cancellous bone. The intervertebral disks were constructed by importing the meshed stereolithography (STL) model into SolidWorks 2022 computer-aided design software (Dassault Systèmes, Providence, RI, USA) and manually modeling a geometric representation of the disk between each vertebra. This geometry was imported into Abaqus 2019, where the annulus fibrosus and nucleus pulposus were manually sectioned. The annulus fibrosus was divided and modeled as a composite solid with alternating $\pm 30^{\circ}$ collagen fiber rebar elements using the "no compression" property. The nucleus pulposus was sectioned and modeled as a linear elastic material. The facet joints were modeled using three-dimensional gap elements with a defined clearance of 0.5 mm. The ligamentous structures of the spine and sacroiliac joints

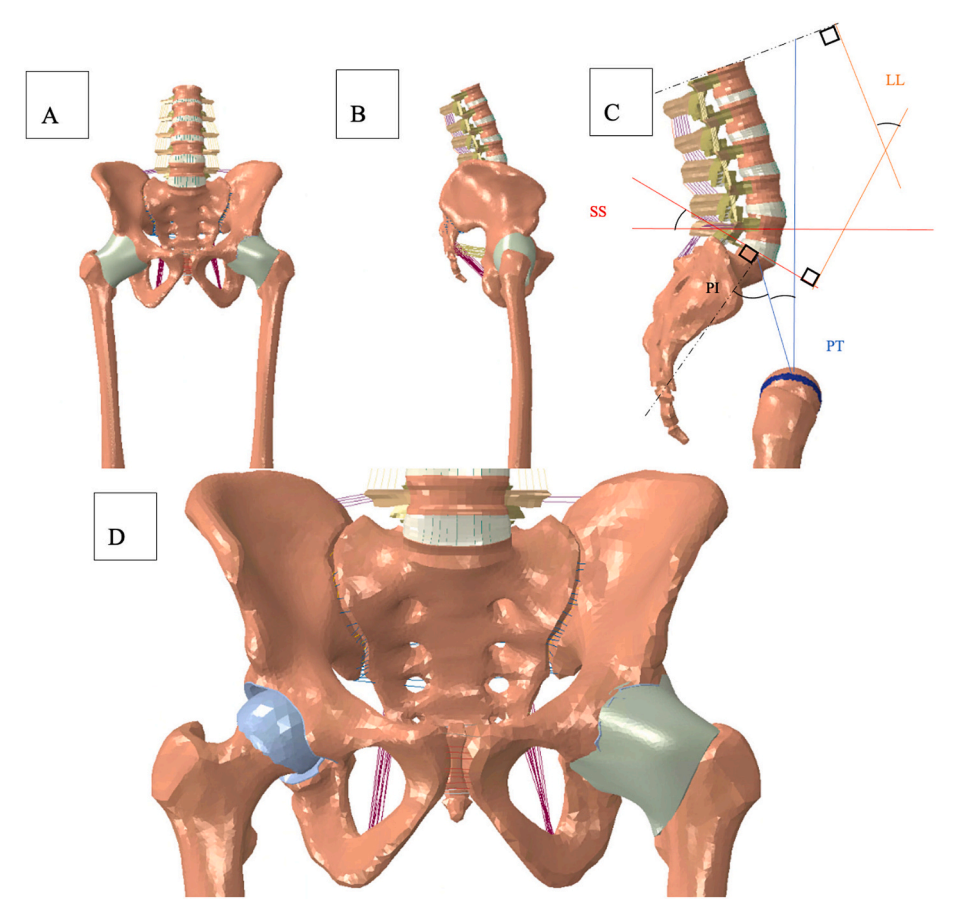


Fig. 1. Finite element model with the following spinopelvic parameters: PI = 46, SS = 26.7, PI = 20, LL = 51. A) Represents the anterior view of the model, B) represents the sagittal profile, C) represents the spinopelvic angle measurements (PT, PI, SS, LL), D) represents the articulating surface of the hip joint with the capsule removed (right hip) and the capsule surrounding the hip joint (left hip).

(SIJ) were modeled as truss elements. Ligament insertions were positioned according to anatomical references to ensure accurate placement. We conducted several range-of-motion validation studies to confirm the validity of the SIJ ligament insertions (Joukar et al., 2018; Joukar et al., 2019; Kumaran et al., 2023). The results verified that our approximations produced realistic motion across the ligament-included segments. Table 1 lists the material properties used in the FE models (Jones, 2013; Palepu, 2013; Panjabi et al., 1994; Seyed Vosoughi et al., 2019). Validation of the vertebral components of the lumbar spine are described elsewhere (Gerber, 2015; Ivanov et al., 2009; Kumaran et al., 2021; Lindsey et al., 2015; Palepu, 2013; Seyed Vosoughi et al., 2019).

2.2. Hip joint creation and validation

The femoral heads were positioned relative to the pelvis according to anatomical parameters described by Wu et al., (Wu et al., 2002). The femoral head and acetabular cartilage were modeled in Abaqus 2019 by creating a 1 mm offset, solid layer of mesh from the surfaces of the femoral head and acetabulum. Hybrid formulation (C3D4H) was applied to this solid mesh layer. The cartilage layer thickness of 1 mm was determined based on measurements from a magnetic resonance imaging study of femoral head and acetabular cartilage conducted by Mechlenburg et al. (Mechlenburg et al., 2007). Ten to twelve random nodal coordinates of the femoral heads and acetebulae were obtained to create a best fit sphere whose centroid coordinates were used to properly place the femoral heads within the acetabulae (Rachakonda, 2023). The cartilage was modeled with incompressible, neoHookean hyperelastic material properties (Anderson et al., 2008). The hip joint was adjusted until the joint space fell within reported parameters determined by Goker et al. (3.43 \pm 0.40 for the right hip and 3.48 \pm 0.68 for the left hip) (Goker et al., 2003). The hip joint capsule was created in Solidworks 2022 based on circumferential locations defined by Stewart et al. (Stewart et al., 2004). Hyperelastic material properties were applied to this geometry based on the Ogden strain energy potential and utilizing uniaxial test data based on a study performed by Stewart et al. (Stewart et al., 2004). Muscles spanning the hip joint from their physiologic origins and insertions were included in the FE model as connector elements with stiffnesses based on Phillips et al. (Table 1) (Phillips et al.,

The growth plate was modeled by sectioning 7 mm of the femoral head (Yadav et al., 2016). The right and left femur physeal-diaphysis angle (PDA) was 39° and 44°, respectively (Fig. 2) (Castro-Abril et al., 2015). Elastic material properties were applied to the growth plate (Table 1) (Castro-Abril et al., 2015; Farzaneh et al., 2015; Fishkin et al., 2006; Paseta et al., 2019). The original model had the following spinopelvic parameters: $SS = 31.7^{\circ}$, $PT = 9.8^{\circ}$, $PI = 41.5^{\circ}$, and $LL = 46^{\circ}$.

This model was modified with various SS and PT angles by rotating the sacrum and pelvis, respectively (Kumaran et al., 2023). The SS angles were incrementally increased by 5° to obtain PIs of 36° , 41° , 46° , and 52° , respectively. To understand the influence of PT on the growth plate, each SS modified model had two variants: high PT (posteriorly tilted) and low PT (anteriorly tilted) cases (Table 2).

2.3. Loads, boundary conditions, and analysis

A 400 N compressive follower load was applied following the curvature of the L1-L5 vertebrae through wire elements to simulate the passive effect of muscle forces and weight of the upper trunk (Joukar et al., 2019). A 500 N force was distributed between the sacral promontory and pubic symphisys to simulate body weight on the pelvis and femur (Joukar et al., 2019). To assess common activities of daily living and their impact on the hip joint and growth plate, two leg stance (2LS), right leg one leg stance (1LS), Ascending stairs heel strike (AHS), descending stairs heel strike (DHS), and walking heel strike (WHS) were simulated. 2LS and 1LS simulated neutral pelvic and femoral positions by fixing the base of the femurs to assess the hip joints in a static posture

Table 1

Material properties assigned to the finite element models (Anderson et al., 2008; Butler et al., 1992; Dalstra et al., 1995; Fishkin et al., 2006; Goel et al., 2005; Henak et al., 2014; Joukar et al., 2018; Joukar et al., 2019; Kumaran et al., 2021; Momeni Shahraki et al., 2015; Paseta et al., 2019; Phillips et al., 2007; Stewart et al., 2004). E represents Young's modulus, y represents Poisson's ratio.

Component	Material Properties	Constitute Relation	Element Type
Vertebral Cortical Bone (Goel et al., 2005)	$\begin{aligned} E &= 12,\!000 \\ MPa \\ v &= 0.3 \end{aligned}$	Isotropic, Elastic	8 Node Brick Element (C3D8)
Vertebral Cancellous Bone (Goel et al., 2005)	E = 100 MPa	Isotropic, Elastic	4 Node Tetrahedral Element (C3D4)
2003)	v = 0.2		Ziellielle (GGZ 1)
Pelvis Cortical Bone (Lindsey et al., 2015)	$\begin{aligned} E &= 17,\!000 \\ MPa \end{aligned}$	Isotropic, Elastic	4 Node Tetrahedral Element (C3D4
	v = 0.3		
Sacrum Cancellous Bone (Lindsey et al., 2015)	Heterogenous	Isotropic, Elastic	4 Node Tetrahedral Element (C3D4)
Ilium Cancellous Bone (Lindsey et al., 2015)	$E=70\;MPa$	Isotropic, Elastic	
Emiliasely et al., 2010)	v = 0.2	Littotic	4 Node
			Tetrahedral
	B 48.000		Element (C3D4)
Femur Cortical Bone (E = 17,000 MPa	Isotropic, Elastic	4 Node Tetrahedral
Anderson et al., 2008)	IVIF a	FIGSUL	Element (C3D4)
" - (v = 0.29		
Femur Cancellous Bone (E = 100 MPa	Isotropic, Elastic	4 Node Tetrahedral
Anderson et al., 2008)		Elastic	Element (C3D4)
	v = 0.2		(222),
Ground Substance of	c10 = 0.035		
Annulus Fibrosis (Momeni Shahraki et al., 2015)	k1 = 0.296	Anisotropic, Hyperelastic (HGO)	8 Node Brick Element (C3D8)
	k2 = 65		
Nucleus Pulposus (Goel et al., 2005)	E = 1 MPa	Isotropic, Elastic	8 Node Brick Element (C3D8)
Hip Cartilage (Anderson	v = 0.499 $C10 = 6.8$	Neo-Hookean,	4 Node
et al., 2008)	D1 = 0.001	Hyperelastic	Tetrahedral, Hybrid Element (C3D4H)
Hip Capsule (Stewart et al., 2004)	Uniaxial Test Data	Ogden, Hyperelastic	4 Node Tetrahedral, Hybrid Element
Growth Plate (Castro-	E = 5 MPa	Isotropic,	(C3D4H) 4 Node
Abril et al., 2015; Farzaneh et al., 2015;	2 0 1111 0	Elastic	Tetrahedral Element (C3D4)
Fishkin et al., 2006; Paseta et al., 2019)	v = 0.49		
Anterior Longitudinal (Goel et al., 2005)	7.8 MPa (<12%), 20 MPa	Non-linear, Hypoelastic	Truss Element (T3D2)
	(>12%)		
Posterior Longitudinal (10 MPa	Non-linear,	Truss Element
Goel et al., 2005)	(<11%), 20 MPa (>11%)	Hypoelastic	(T3D2)
Ligamentum Flavum (15 MPa	Non-linear,	Truss Element
Goel et al., 2005)	(<6.2%), 19.5 MPa (>6.2%)	Hypoelastic	(T3D2)
Intertransverse (Goel	10 MPa	Non-linear,	Truss Element
intertransverse (Goet	(<18%),	Hypoelastic	(T3D2)
et al., 2005)	58.7 MPa		
et al., 2005)	(>18%)	NT 11	m vi
		Non-linear, Hypoelastic	Truss Element (T3D2)

(continued on next page)

Table 1 (continued)

Component	Material Properties	Constitute Relation	Element Type
Supraspinous (Goel et al., 2005)	8 MPa (<20%), 15 MPa (>20%)	Non-linear, Hypoelastic	Truss Element (T3D2)
Capsular (Goel et al., 2005)	7.5 MPa (<25%), 32.9 MPa (>25%)	Non-linear, Hypoelastic	Truss Element (T3D2)
Anterior SIJ (Butler et al., 1992)	125 MPa (5%), 325 MPa (>10%), 316	Non-linear, Hypoelastic	Truss Element (T3D2)
Short Posterior SI (Butler et al., 1992)	MPa (>15%) 43 MPa (5%), 113 MPa (>10%), 110	Non-linear, Hypoelastic	Truss Element (T3D2)
Long Posterior SI (Butler et al., 1992)	MPa (>15%) 150 MPa (5%), 391 MPa (>10%), 381	Non-linear, Hypoelastic	Truss Element (T3D2)
Interosseous (Butler et al., 1992)	MPa (>15%) 40 MPa (5%), 105 MPa (>10%), 102	Non-linear, Hypoelastic	Truss Element (T3D2)
Sacrospinous (Butler et al., 1992)	MPa (>15%) 304 MPa (5%), 792 MPa (>10%), 771 MPa (>15%)	Non-linear, Hypoelastic	Truss Element (T3D2)
Sacrotuberous Ligament (Butler et al., 1992)	326 MPa (5%), 848 MPa (>10%), 826 MPa (>15%)	Non-linear, Hypoelastic	Truss Element (T3D2)
Gluteus Maximus (Phillips et al., 2007) Gluteus Medius (Phillips et al., 2007) Gluteus Minimus (Phillips et al., 2007) Psoas Major (Phillips et al., 2007) Adductor Magnus (Phillips et al., 2007) Adductor Longus (Phillips et al., 2007)	$\begin{split} k &= 344 \text{ N/} \\ mm \\ k &= 779 \text{ N/} \\ mm \\ k &= 660 \text{ N/} \\ mm \\ k &= 100 \text{ N/} \\ mm \\ k &= 257 \text{ N/} \\ mm \\ k &= 134 \text{ N/} \\ mm \end{split}$		Connector Element Connector Element Connector Element Connector Element Connector Element Connector Element
Adductor Brevis (Phillips et al., 2007)	$\begin{array}{l} k = 499 \; N/\\ mm \end{array}$		Connector Element

(Joukar et al., 2019). To simulate AHS, DHS, and WHS, the femurs and pelvis were reoriented to match *in-vivo* kinematic hip joint data. WHS corresponded to the peak contact force in heal strike during the gait cycle, whereas AHS and DHS corresponded to force peaks during stairs ascent and descent, respectively (Bergmann et al., 2001). Average contact stress and contact area of the femoral head was calculated for each motion and alignment. To evaluate shear stresses on the proximal femoral growth plate, maximum Tresca stresses were recorded.

3. Results

To assess and validate proper functionality of the hip joints, contact stresses and areas were evaluated based on simulated positions corresponding to two-leg stance (2LS), walking heel strike (WHS), ascending stairs heel strike (AHS), and descending stairs heel strike (DHS) per femur angles based on Bergmann et al.'s data (Bergmann et al., 2001; Joukar et al., 2019). Peak and average contact stresses (MPa) and contact area (mm²) at the hip joint were compared to previous studies by simulating their benchtop protocols (Anderson et al., 2008; Harris et al.,

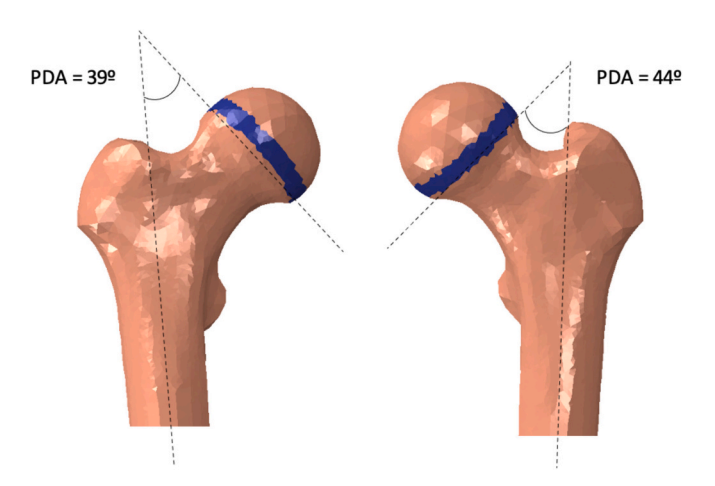


Fig. 2. Representation of the right and left femurs with 7 mm thick growth plates. The PDA for the right and left femurs were 39° and 44° , respectively. The PDA was measured by drawing a line through the intremedullary canal in the femur and an intersecting line parallel to the base of the epiphyseal growth plate.

Table 2Spinopelvic parameters of the finite element models. Low PT refers to anteriorly tilted pelvi, whereas high PT refers to posterior pelvic tilt.

Model	Pelvic Incidence (PI°)	Sacral Slope (SS°)	Pelvic Tilt (PT°)	Lumbar Lordosis (LL°)
Model 1	36°	26.7°	9.5°	41°
Model 2	36°	16.7°	19.5°	41°
Model 3	41°	31.7°	9.8°	46°
Model 4	41°	21.7°	19.8°	46°
Model 5	46°	36.7°	10°	51°
Model 6	46°	26.7°	20°	51°
Model 7	52°	41.7°	10.4°	56°
Model 8	52°	31.7°	20.4°	56°

2012; Joukar et al., 2019). Average contact stresses were found to be in range of previous studies with peak contact stresses being slightly higher. Regarding contact areas, values were in-line of previous studies. The protocol and results for validation are outlined in the supplementary material file.

Overall, higher PT indicated larger contact areas compared to low PT variants. A combination of higher PT and PI resulted in substantially larger contact areas compared to low PT and low PI for each simulated motion (\sim 18% increases) (Fig. 3).

Regarding hip contact stresses, heel strike simulations (WHS, AHS, and DHS) resulted in the largest values compared to 2LS and 1LS, especially in the PI41 cases. The 1LS and 2LS simulations showed that as PT increased, larger contact stresses were mitigated (Fig. 4). All heel strike simulations indicated a similar trend with higher contact stresses in the high PT variants (~10% increases), except for WHS. In WHS, PI41-High PT resulted in the largest contact stress with marginal changes in higher PIs. AHS indicated lower contact stresses in PI52 compared to all other cases in AHS, with PI46 indicating the largest contact stress. In DHS, PI41 resulted in the largest contact stresses compared to the other cases.

Regarding Tresca stresses, heel strike simulations resulted in the largest stresses on the growth plate with AHS indicating the largest

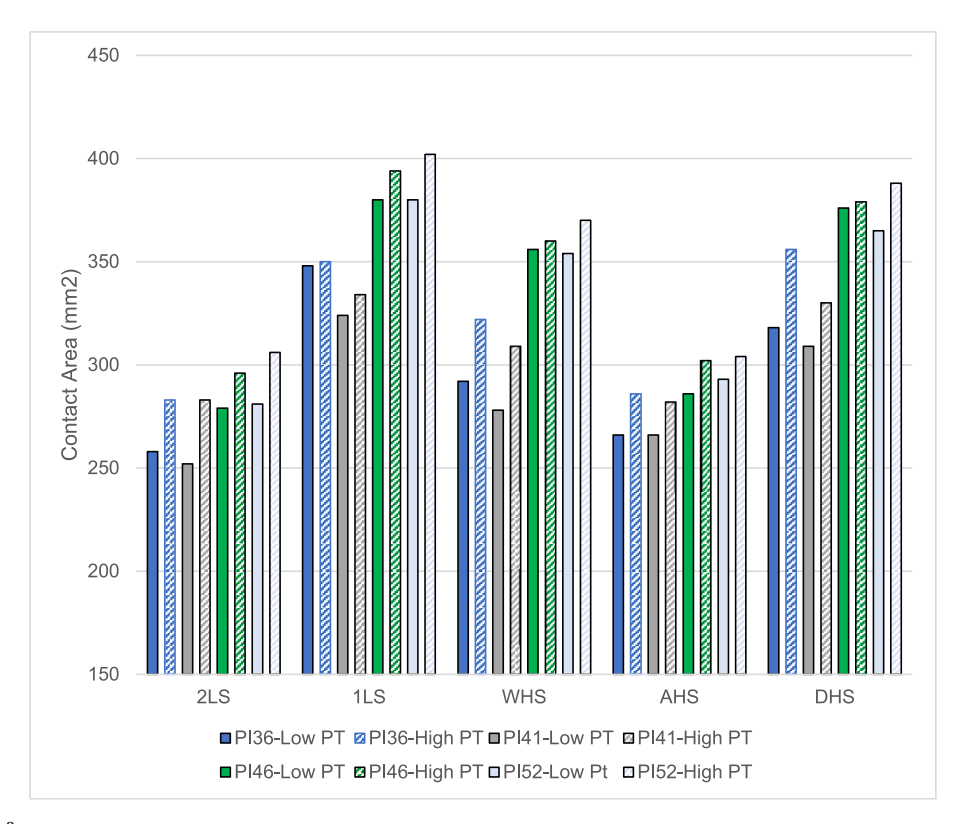


Fig. 3. Contact area (mm²) on the femoral head cartilage in various stances for low pelvic tilt (solid bar) and high pelvic tilt (hashed bar) variants. 2LS refers to two leg stance, 1LS refers to one leg stance, WHS refers to walking heel-strike, AHS refers to ascending stairs heel strike, and DHS refers to descending stairs heel strike.

values overall. High PT variants resulted in larger shear stresses compared to the low PT variants (~18% increases) except in 2LS. A combination of high PT and PI resulted in the largest overall Tresca stress on the growth plate for each simulated case (10–24% increases) (Fig. 5). In 1LS, WHS, AHS and DHS, Tresca stresses for the high PT variant of PI36 was comparable to PI46-High PT, though smaller than PI52-High PT.

4. Discussion

The aim of the current study was to elucidate the role of spinopelvic parameters on the hip joint and an open femoral growth plate to assess the potential for development of SCFE. Current research in this area is limited, with only a few studies leveraging FE models to examine SCFE under various loading scenarios (Castro-Abril et al., 2015; Farzaneh et al., 2015; Fishkin et al., 2006; Paseta et al., 2019; Rhyu et al., 2011; Shah, 2005). Our findings revealed that a combination of posterior pelvic tilt (PT) and high pelvic incidence (PI) angles lead to large hip contact area (Fig. 6) and elevated shear stresses on the proximal femoral physis.

Previous reports have stated that higher pelvic incidence and sacral slope angles contribute to larger mechanical stresses on the hip joint (Gebhart et al., 2016; Kumaran et al., 2023). Lazennec and colleagues described clinical consequences of sagittal imbalance in pelvic and subpelvic regions in patients and eluded to how atypical postures and morphology contribute to disturbances in the hip joint (Lazennec et al., 2007; Lazennec et al., 2011). Disruption of the spinopelvic complex displaces mechanical forces and increases load absorption on the intervertebral discs and femoroacetabular joints. The present study suggests that various spinopelvic alignments distribute stresses at the hip joint and growth plate differently, specifically patients with high pelvic incidence and posterior pelvic tilt may be more prone to SCFE (Zupanc et al., 2008).

Conflicting results are present in the current literature regarding PI

and SCFE. An adult cadaveric study assessing bone morphology performed by Gebhart et al. identified lower PI in post-SCFE specimens compared to a control of normal specimens (Gebhart et al., 2015) (Bao et al., 2018; Negrini et al., 2022). Our results indicate that lower pelvic incidence angles contribute to larger contact stress at the hip joint, and seldom to shear stresses on the epiphyseal growth plate, which are two components that are risk factors for SCFE (Zupanc et al., 2008). Additionally, the type of activity performed and degree of pelvic tilt also determine the overall shear at the growth plate. For instance, some postures indicated that low pelvic incidence combined with posterior pelvic tilt (PI36-HighPT) contributed to shear at the growth plate more than higher pelvic incidence (PI46). However, in most postures, high pelvic incidence alone and posterior pelvic tilt combined with high pelvic incidence resulted in the largest shear at the growth plate. This finding can be attributed to the high sacral slope and lumbar lordosis angles distributing a shear load through the femur and proximal femoral growth plate. Contrast this to the low pelvic incidence cases where the model remains more vertical due to a low sacral slope, the load distributing from the lumbar spine through the femoro-acetabular joint and growth plate were likely compressive forces rather than shear.

A retrospective, observational study by Wako et al. did not identify a relationship between PI and SCFE, though determined a significance in retroverted acetabuli and excessive coverage of the anterior and superior acetabulum in SCFE patients compared to a control group (Wako et al., 2020). Current studies have mixed results on whether SCFE-affected hips are associated with the phenomena of anteversion or retroversion (Bauer et al., 2013; Gebhart et al., 2015; Sankar et al., 2011; Wako et al., 2020). Additionally, many studies do not correct for pelvic tilt which has the potential to overestimate acetabular version (Monazzam et al., 2013; Siebenrock et al., 2003). In the current study, two pelvic tilt variants were examined for posterior and anterior pelvic tilt. Results indicated high contact area in the posterior pelvic tilt variants compared to anterior tilt which can be attributed to larger coverage of the posterior femoral head with the superior acetabulum. Contact

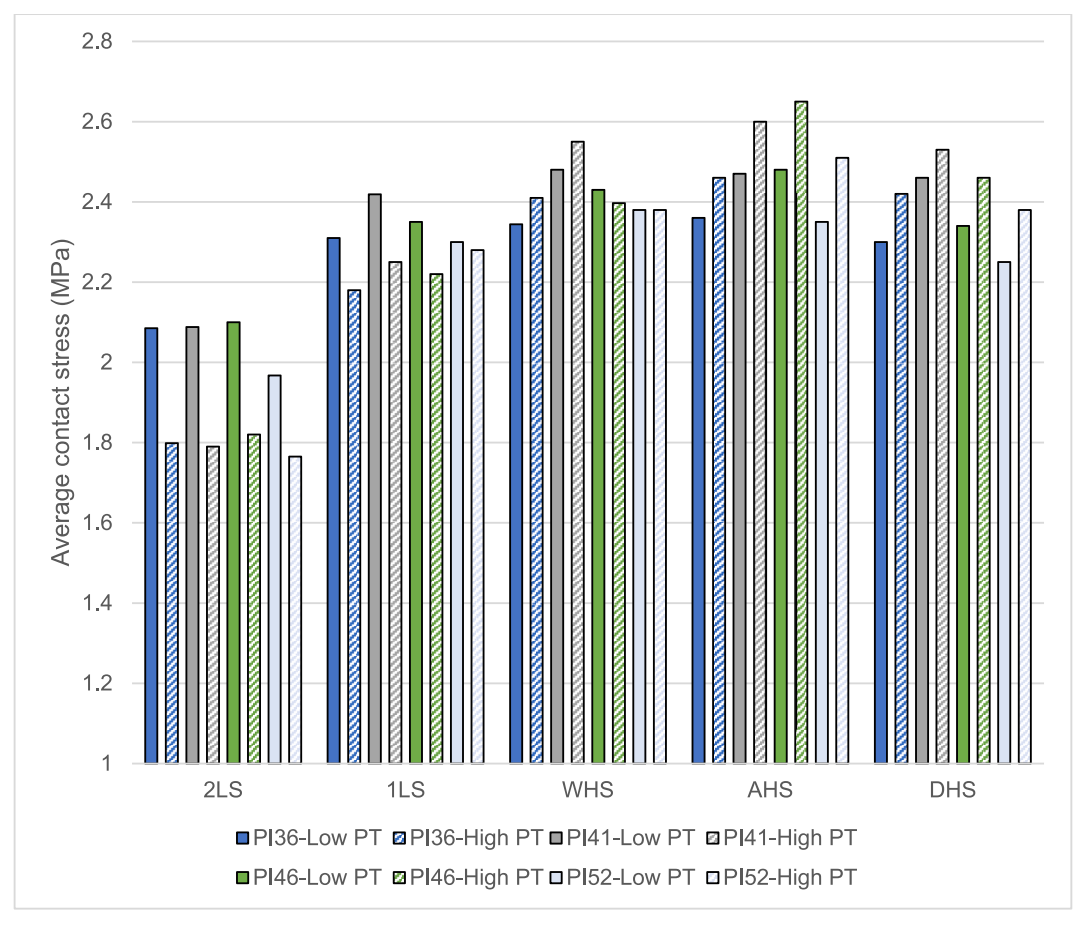


Fig. 4. Average hip contact stress (MPa) on the femoral head cartilage in various stances for low pelvic tilt (solid bar) and high pelvic tilt (hashed bar) variants.

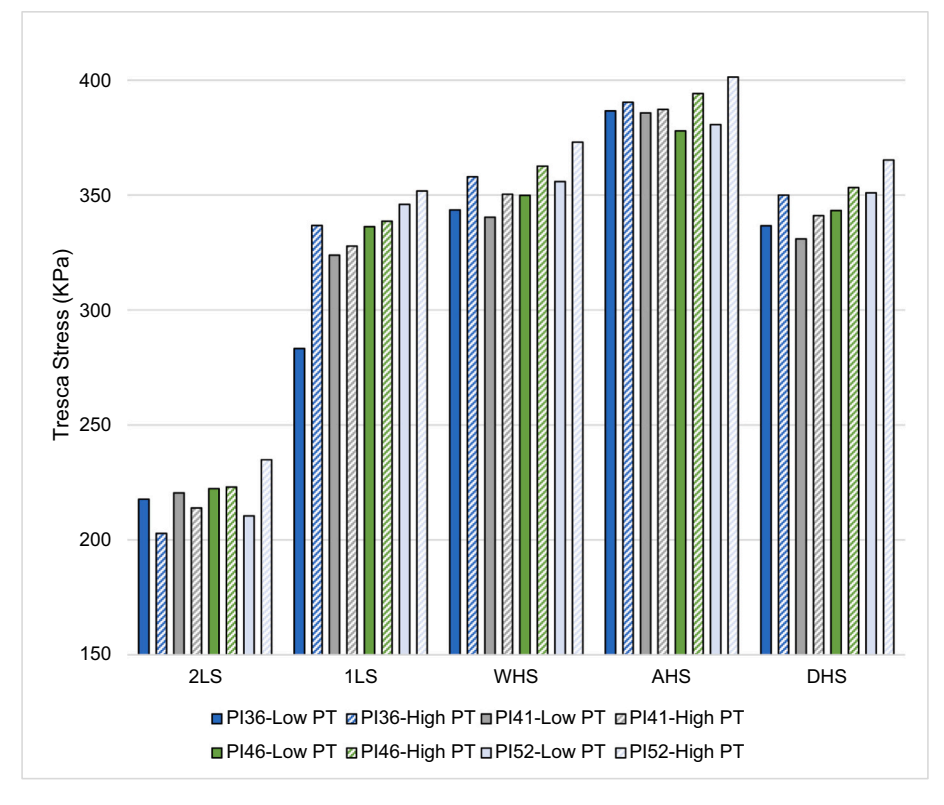


Fig. 5. Maximum Tresca (shear) stress in KPa on the growth plate in various stances for low pelvic tilt (solid bar) and high pelvic tilt (hashed bar) variants.

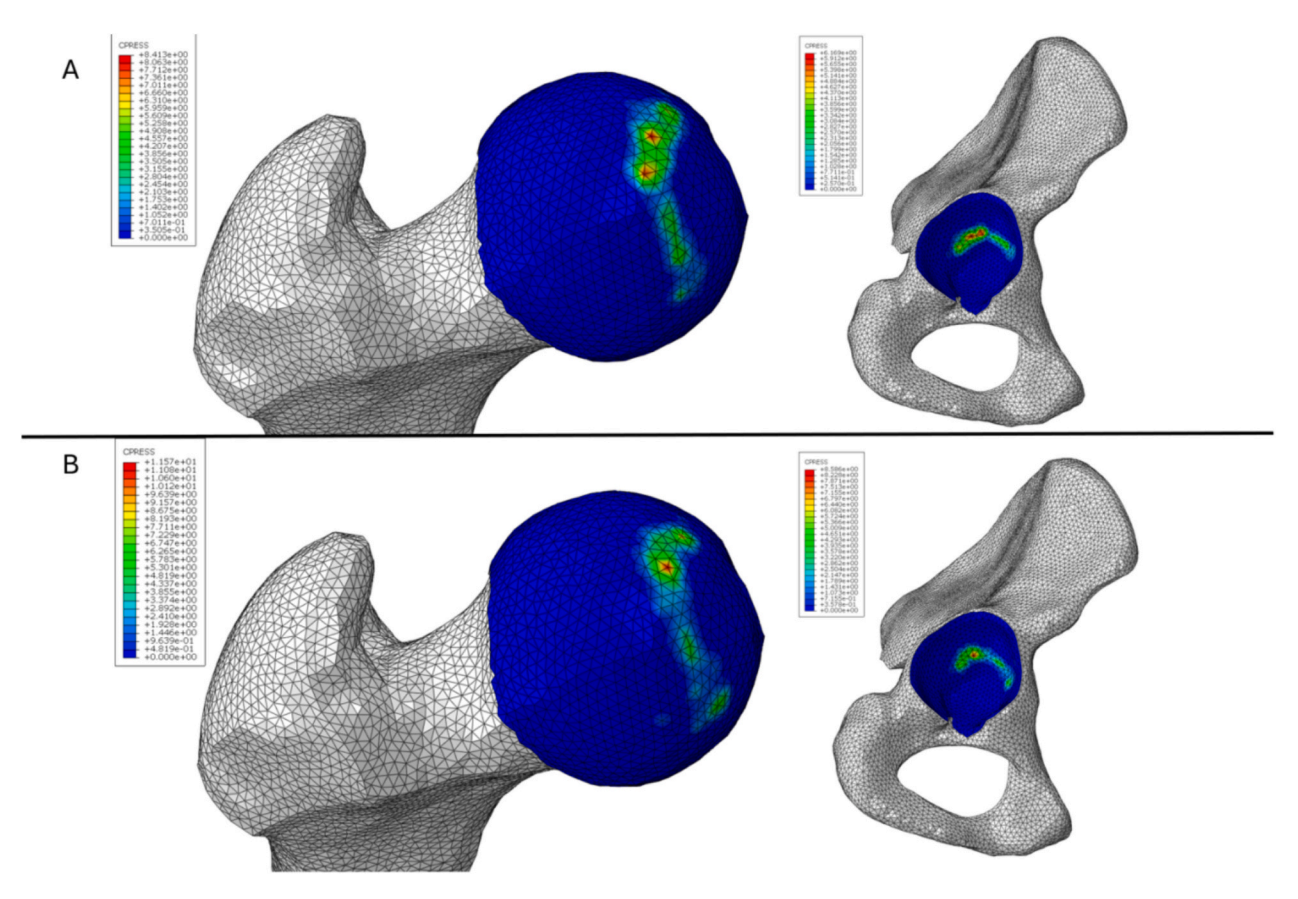


Fig. 6. Contact pressure contours for the femoral head and acetabular cartilage are shown for two alignments, (A) PI46-Low PT and (B) PI46-High PT during the ascending stairs heel strike (AHS) loading condition. Maximum contact pressures on the femoral head and acetabulum were higher in (B) for both the femoral head and acetabular cartilage compared to (A). An irregularly shaped, monocentric contact pattern on the femoral head was observed for AHS (Anderson et al., 2008).

stresses resulted in the same trend in 2LS and 1LS, though the opposite was seen in walking, ascending stairs, and descending stairs as posterior tilted variants indicated higher contact stress. Since stress is defined as the force applied over a certain area, this may seen counterintuitive, though as described by Henak et al., contact location, distribution and direction change during walking, ascending stairs, and descending stairs. In our case, the anterior tilted pelvi along with the angles of the femur in the heel strike simulations distributed the load anteriorly and superiorly compared to posterior tilt, thus agreeing with Henak and colleagues' findings (Henak et al., 2014). Our results suggest that patients may experience higher contact stress on the femoral head cartilage during gait, especially in patients with excess posterior pelvic tilt (Henak et al., 2014; Hesper et al., 2017; Monazzam et al., 2013; Song et al., 2021; Wako et al., 2020). Along with higher femoral head contact stress, patients with posterior pelvic tilt may be more prone to slip due to higher shear stresses at the growth plate. We recommend that future biomechanical studies include morphological parameters like the lateral center edge angle (LCEA), which measures the coverage of the femoral head by the acetabulum, and the alpha angle, which assesses the sphericity of the femoral head-neck junction. This will help clarify how acetabular coverage and femoral head morphology mechanically contribute to asymmetric loading of the hip joint and growth plate (Boyle et al., 2016; Kitadai et al., 1999).

In the adult population, atypical pelvic postures produce consequences to the stability of the hip after arthroplasty, contributing further to imbalance of sagittal spinopelvic parameters (Lazennec et al., 2007; Lazennec et al., 2011). Furthermore, high pelvic incidence has been suggested to contribute to excessive loading on the femoral head cartilage leading to osteoarthritis of the hip (Gebhart et al., 2016; Maurer et al., 2023; Yoshimoto et al., 2005). Regarding SCFE, osteoarthritis has

remained a problematic sequealae in young adult patients who experienced severe slip or surgical pinning to repair the proximal femoral physis (Abraham et al., 2007; Wiemann and Herrera-Soto, 2013). Long term follow-up of these patients commonly exhibit hip cartilage degeneration due to CAM deformity and femoroacetabular impingement (de Poorter et al., 2016; Helgesson et al., 2018).

More recently, a gait analysis conducted by Sklensky et al. assessed the hip-spine relationship in 23 pediatric patients with Lenke type 1 idiopathic scoliosis. Interestingly, they identified that two-thirds of their subjects exhibited asymmetrical hip loading (i.e. higher hip loading on one hip compared to the contralateral hip) (Sklensky et al., 2022). Their results suggests that the translation of the apical thoracic vertebrae and coronal imbalance are related to asymmetric hip loading. As a result of this imbalance, lumbar lordosis was identified to play a compensatory role in establishing symmetrical loading of the hips. While our study did not directly investigate the link between asymmetric hip loading and SCFE, the concept that altered loading conditions and compensatory mechanisms—such as those seen in asymmetric gait patterns—may contribute to the development or exacerbation of SCFE is plausible. Altered gait and hip-spine loading in scoliosis, could theoretically exacerbate this vulnerability, particularly under asymmetrical loads. Based on these previous findings and the current study's results, a pediatric patient's dynamic mechanical history, surgical history of pinning, and sagittal alignment may suggest a compounding deleterious effect on the hip cartilage and early-onset osteoarthritis in sagittally imbalanced patients (Brand, 2005). Further research using specific biomechanical models that account for these asymmetries could provide deeper insights. Such studies might investigate whether specific alterations in gait or spinal alignment contribute to the mechanical environment that predisposes individuals to SCFE.

The current study's finite element (FE) model, while insightful, is subject to certain limitations. Notably, we employed an adult model in this theoretical analysis. This decision was influenced by the fact that cadaver studies extensively document the hip-spine relationship in adults but not in children (Anderson et al., 2008; Harris et al., 2012; Joukar et al., 2019). Additionally, SCFE can occur in adults, albeit rarely, providing further rationale for using an adult model (Huang et al., 2019; Niu et al., 2021; Speirs et al., 2019). Part of the decision to utilize an adult model stemmed from the fact that CT imaging for pediatric SCFE patients often focuses solely on the pelvic area, excluding critical details like lumbar lordosis and sacral slope. Conducting additional spine-focused CT scans would unnecessarily expose children to extra radiation. Consequently, crafting patient-specific models encompassing the complete spinopelvic complex with varied spinal alignments in pediatric SCFE patients necessitated certain simplifications. While it's recognized that pelvic and spinal morphology evolve from childhood through adulthood, the study's results suggest a potential mechanical linkage between spinopelvic parameters and the proximal femoral growth plate. The absence of validated pediatric spine models in the literature, predominantly due to the lack of pediatric cadaver studies, further justified our approach. Additionally, while the reference range for pelvic incidence (PI) in adults spans from 33° to 85°, our study faced a technical limitation in that our finite element (FE) model could only simulate PIs between 36° and 51° (Chen and Zhao, 2018). This restriction was due to element penetration and contact errors encountered when attempting to adjust the PI beyond 51°. As a result, the range of PIs explored in our study was narrower than ideal. This constraint potentially limits the generalizability of our findings across the full spectrum of PI values typically observed in clinical settings. Muscle forces spanning the hip and spine were simplified as passive connector elements with elastic properties and follower loads. Global mechanics were of interest to the authors rather than micro-mechanics, therefore the growth plate was simulated as a linear, elastic material property (Farzaneh et al., 2015; Fishkin et al., 2006; Paseta et al., 2019). Additionally, the physeal-disphyseal angle and physeal thickness were held constant due to variation of plate thickness and angle having little contribution to stresses on the growth plate (Castro-Abril et al., 2015; Fishkin et al., 2006; Shah, 2005). Lastly, only a male model was constructed in this study. The biomechanics of female pelvi may distribute loads differently compared to male pelvi, therefore future studies should examine how sexual dimorphism contributes to SCFE.

5. Conclusion

This study suggests that altered sagittal alignments such as low pelvic incidences in some activities and high pelvic incidences combined with posterior tilted pelvi, may be more prone to slip due to changes in contact stresses at the femoral head and high shear stress on the proximal femoral growth plate. It may be necessary for hip preservation surgeons to consider sagittal imbalance as a potential risk factor for SCFE, though future studies are required to confirm this theory.

CRediT authorship contribution statement

Yogesh Kumaran: Writing – review & editing, Writing – original draft, Visualization, Validation, Resources, Methodology, Investigation, Funding acquisition, Formal analysis, Data curation, Conceptualization. Muzammil Mumtaz: Writing – review & editing, Writing – original draft, Validation, Investigation, Formal analysis, Data curation. Carmen Quatman: Writing – review & editing, Writing – original draft, Supervision, Conceptualization. Julie Balch-Samora: Writing – review & editing, Writing – original draft, Supervision, Investigation. Sophia Soehnlen: Writing – review & editing, Writing – original draft, Validation, Methodology, Investigation, Formal analysis, Data curation, Conceptualization. Brett Hoffman: Writing – review & editing, Writing – original draft, Data curation. Sudharshan Tripathi: Writing – review

& editing, Validation, Methodology, Formal analysis, Data curation, Conceptualization. Norihiro Nishida: Writing – review & editing, Writing – original draft, Supervision, Conceptualization. Vijay K. Goel: Writing – review & editing, Writing – original draft, Supervision, Funding acquisition.

Declaration of competing interest

The authors declare that they have no known competing financial interests or personal relationships that could have appeared to influence the work reported in this paper.

Acknowledgement

This work was partially funded by a United States National Science Foundation (NSF) Industry/University Cooperative Research Center called the Center for Disruptive Musculoskeletal Innovations (CDMI) (IIP-1916629) at the University of California at San Francisco, CA, the Ohio State University, Columbus, OH, and the University of Toledo, Toledo, OH (www.nsfcdmi.org).

Appendix A. Supplementary data

Supplementary data for this article can be found online at https://do i.org/10.1016/j.clinbiomech.2024.106269.

References

- Abraham, E., et al., 2007. Clinical implications of anatomical Wear characteristics in slipped capital femoral epiphysis and primary osteoarthritis. J. Pediatr. Orthop. 27 (7), 788–795.
- Anderson, A.E., et al., 2008. Validation of finite element predictions of cartilage contact pressure in the human hip joint. J. Biomech. Eng. 130 (5), 051008.
- Balch Samora, J., et al., 2018. MRI in idiopathic, stable, slipped capital femoral epiphysis: evaluation of contralateral pre-slip. J. Child. Orthop. 12 (5), 454–460.
- Bao, H., et al., 2018. Lumbosacral stress and age may contribute to increased pelvic incidence: an analysis of 1625 adults. Eur. Spine J. 27 (2), 482–488.
- Bauer, J.P., Roy, D.R., Thomas, S.S., 2013. Acetabular retroversion in post slipped capital femoral epiphysis deformity. J. Child. Orthop. 7 (2), 91–94.
- Bergmann, G., et al., 2001. Hip contact forces and gait patterns from routine activities.
 J. Biomech. 34 (7), 859–871.
 Boyle, M.J., et al., 2016. The alpha angle as a predictor of contralateral slipped capital
- femoral epiphysis. J. Child. Orthop. 10 (3), 201–207.
 Brand, R.A., 2005. Joint contact stress: a reasonable surrogate for biological processes?
- Iowa Orthop. J. 25, 82–94.
- Butler, D.L., et al., 1992. Location-dependent variations in the material properties of the anterior cruciate ligament. J. Biomech. 25 (5), 511–518.
- Castro-Abril, H.A., Galván, F., Garzón-Alvarado, D.A., 2015. Geometrical and mechanical factors that influence slipped capital femoral epiphysis: a finite element study. J. Pediatr. Orthop. B 24 (5), 418–424.
- Chen, H.-F., Zhao, C.-Q., 2018. Pelvic incidence variation among individuals: functional influence versus genetic determinism. J. Orthop. Surg. Res. 13 (1), 59.
- Cignoni, P., Corsini, M.C.M., Dellepiane, M., Ganovelli, F., Ranzuglia, G., 2008. MeshLab: an Open-Source Mesh Processing Tool. In: Sixth Eurographics Italian Chapter Conference, pp. 129–136.
- Dalstra, M., Huiskes, R., van Erning, L., 1995. Development and validation of a threedimensional finite element model of the pelvic bone. J. Biomech. Eng. 117 (3), 272–278.
- de Poorter, J.J., et al., 2016. Long-term outcomes of slipped capital femoral epiphysis treated with in situ pinning. J. Child. Orthop. 10 (5), 371–379.
- Farzaneh, S., Paseta, O., Gomez-Benito, M.J., 2015. Multi-scale finite element model of growth plate damage during the development of slipped capital femoral epiphysis. Biomech. Model. Mechanobiol. 14 (2), 371–385.
- Fishkin, Z., et al., 2006. Proximal femoral physis shear in slipped capital femoral epiphysis–a finite element study. J. Pediatr. Orthop. 26 (3), 291–294.
- Gebhart, J.J., et al., 2015. Pelvic incidence and acetabular version in slipped capital femoral epiphysis. J. Pediatr. Orthop. 35 (6), 565–570.
- Gebhart, J.J., et al., 2016. Relationship between pelvic incidence and osteoarthritis of the hip. Bone & Joint Res. 5 (2), 66–72.
- Gerber, J., 2015. Biomechanical evaluation of Facet Bone Dowels in the Lumbar Spine. In: Department of Bioengineering. University of Toledo: University of Toledo, p. 128.
- Ghobrial, G.M., Al-Saiegh, F., Heller, J., 2018. Procedure 31 spinopelvic balance: Preoperative planning and calculation. In: Operative Techniques: Spine Surgery. Elsevier, pp. 281–287.
- Goel, V.K., et al., 2005. Effects of charite artificial disc on the implanted and adjacent spinal segments mechanics using a hybrid testing protocol. Spine (Phila Pa 1976) 30 (24), 2755–2764.

- Goker, B., et al., 2003. The radiographic joint space width in clinically normal hips: effects of age, gender and physical parameters. Osteoarthr. Cartil. 11 (5), 328–334.
- Haider, S., Podeszwa, D.A., Morris, W.Z., 2022. The etiology and Management of Slipped Capital Femoral Epiphysis: current concept review. J. Pediatr. Orthopaed. Soc. North America 4(4).
- Harris, M.D., et al., 2012. Finite element prediction of cartilage contact stresses in normal human hips. J. Orthop. Res. 30 (7), 1133–1139.
- Helgesson, L., et al., 2018. Early osteoarthritis after slipped capital femoral epiphysis. Acta Orthop. 89 (2), 222–228.
- Henak, C.R., et al., 2014. Patient-specific analysis of cartilage and labrum mechanics in human hips with acetabular dysplasia. Osteoarthr. Cartil. 22 (2), 210–217.
- Hesper, T., et al., 2017. Acetabular retroversion, but not increased acetabular depth or coverage, in slipped capital femoral epiphysis: a matched-cohort study. JBJS 99 (12), 1022–1029.
- Huang, Y.F., et al., 2019. Slipped capital femoral epiphysis in an adult with congenital hypopituitarism: a case report. Medicine (Baltimore) 98 (3), e13997.
- Ivanov, A.A., et al., 2009. Lumbar fusion leads to increases in angular motion and stress across sacroiliac joint: a finite element study. Spine (Phila Pa 1976) 34 (5), E162–E169.
- Jones, A., 2013. Biomechanical and Finite Element Analyses of Alternative Cements for use in Vertebral. In: Department of Bioengineering, 125. University of Toledo: University of Toledo.
- Joukar, A., et al., 2018. Sex specific sacroiliac joint biomechanics during standing upright: a finite element study. Spine (Phila Pa 1976) 43 (18), E1053–E1060.
- Joukar, A., et al., 2019. Effects on hip stress following sacroiliac joint fixation: a finite element study. JOR Spine 2 (4), e1067.
- Kitadai, H.K., et al., 1999. Wiberg's center-edge angle in patients with slipped capital femoral epiphysis. J. Pediatr. Orthop. 19 (1), 97–105.
- Kumaran, Y., et al., 2021. Iatrogenic muscle damage in transforaminal lumbar interbody fusion and adjacent segment degeneration: a comparative finite element analysis of open and minimally invasive surgeries. Eur. Spine J. 30 (9), 2622–2630.
- Kumaran, Y., et al., 2023. Effects of sacral slope changes on the intervertebral disc and hip joint: a finite element analysis. World Neurosurg, 176, e32–e39.
- Lazennec, J.Y., et al., 2007. Hip spine relationships: application to total hip arthroplasty. Hip Int. 17 (Suppl. 5), S91–104.
- Lazennec, J.Y., Brusson, A., Rousseau, M.A., 2011. Hip-spine relations and sagittal balance clinical consequences. Eur. Spine J. 20 Suppl 5 (Suppl. 5), 686–698.
- Le Huec, J.C., et al., 2011. Pelvic parameters: origin and significance. Eur. Spine J. 20 Suppl 5 (Suppl. 5), 564–571.
- Legaye, J., et al., 1998. Pelvic incidence: a fundamental pelvic parameter for threedimensional regulation of spinal sagittal curves. Eur. Spine J. 7 (2), 99–103.
- Lehmann, C.L., et al., 2006. The epidemiology of slipped capital femoral epiphysis: an update. J. Pediatr. Orthop. 26 (3), 286–290.
- Lindsey, D.P., et al., 2015. Sacroiliac joint fusion minimally affects adjacent lumbar segment motion: a finite element study. Int. J. Spine Surg. 9, 64.
- Loder, R.T., Skopelja, E.N., 2011. The epidemiology and demographics of slipped capital femoral epiphysis. ISRN Orthop. 2011, 486512.
- maurer, E., et al., 2023. Lack of correlation between hip osteoarthritis and anatomical
- spinopelvic parameters obtained in supine position on MRI. Injury 54 (2), 525–532. Mechlenburg, I., et al., 2007. Cartilage thickness in the hip joint measured by MRI and stereology–a methodological study. Osteoarthr. Cartil. 15 (4), 366–371.
- Momeni Shahraki, N., et al., 2015. On the use of biaxial properties in modeling annulus as a Holzapfel-gasser-Ogden material. Front. Bioeng. Biotechnol. 3, 69.
- Monazzam, S., et al., 2013. Is the acetabulum Retroverted in slipped capital femoral epiphysis? Clin. Orthop. Relat. Res. 471 (7), 2145–2150.
- Negrini, S., et al., 2022. Sagittal balance in children: reference values of the sacral slope for the Roussouly classification and of the pelvic incidence for a new, age-specific classification. Appl. Sci.-Basel 12 (8).
- Niu, Z., et al., 2021. Slipped capital femoral epiphysis with hypopituitarism in adults: a case report and literature review. Medicine (Baltimore) 100 (51), e28256.
- Novais, E.N., Millis, M.B., 2012. Slipped capital femoral epiphysis: prevalence, pathogenesis, and natural history. Clin. Orthop. Relat. Res. 470 (12), 3432–3438.

- Palepu, V., 2013. A thesis entitled biomechanical effects of initial occupant seated posture during rear end impact injury. In: Department of Bioengineering. University of Toledo.
- Panjabi, M.M., et al., 1994. Mechanical behavior of the human lumbar and lumbosacral spine as shown by three-dimensional load-displacement curves. J. Bone Joint Surg. Am. 76 (3), 413–424.
- Paseta, O., et al., 2019. Parametric geometrical subject-specific finite element models of the proximal femur: a tool to predict slipped capital femoral epiphyses. Int. J. Computat. Vision Biomechan. 5.
- Phillips, A.T., et al., 2007. Finite element modelling of the pelvis: inclusion of muscular and ligamentous boundary conditions. Med. Eng. Phys. 29 (7), 739–748.
- Polly, D.W., et al., 2012. Chapter 31 pediatric and adult scoliosis. In: Ellenbogen, R.G., Abdulrauf, S.I., Sekhar, L.N. (Eds.), Principles of Neurological Surgery (Third Edition). W.B. Saunders, Philadelphia, pp. 497–507.
- Rachakonda, P., 2023. Sphere Fit. In: MATLAB Central File Exchange. MATLAB Central File Exchange.
- Rhyu, K.H., et al., 2011. Application of finite element analysis in pre-operative planning for deformity correction of abnormal hip joints a case series. Proc. Inst. Mech. Eng. H J. Eng. Med. 225 (9), 929–936.
- Roussouly, P., et al., 2006. The vertical projection of the sum of the ground reactive forces of a standing patient is not the same as the C7 plumb line: a radiographic study of the sagittal alignment of 153 asymptomatic volunteers. Spine (Phila Pa 1976) 31 (11), E320–E325.
- Sankar, W.N., et al., 2011. Acetabular morphology in slipped capital femoral epiphysis. J. Pediatr. Orthop. 31 (3), 254–258.
- Schwab, F., et al., 2006. Gravity line analysis in adult volunteers: age-related correlation with spinal parameters, pelvic parameters, and foot position. Spine (Phila Pa 1976) 31 (25), E959–E967.
- Seyed Vosoughi, A., et al., 2019. Optimal satellite rod constructs to mitigate rod failure following pedicle subtraction osteotomy (PSO): a finite element study. Spine J. 19 (5), 931–941.
- Shah, H.H., 2005. A Finite Element Study of Slipped Capital Femoral Epiphysis (SCFE). State University of New York at Buffalo, United States – New York, p. 70.
- Siebenrock, K.A., Kalbermatten, D.F., Ganz, R., 2003. Effect of pelvic tilt on acetabular retroversion: a study of Pelves from cadavers. Clin. Orthop. Relat. Res. 407, 241–248.
- Sklensky, J., et al., 2022. The relationship of hip loading asymmetry and radiological parameters of the spine in Lenke type 1 idiopathic scoliosis. Gait Posture 94, 160–165.
- Song, S.K., et al., 2021. Changes of acetabular anteversion according to pelvic tilt on sagittal plane under various acetabular inclinations. J. Orthop. Res. 39 (4), 806–812.
- Speirs, J.N., Morris, S.C., Morrison, M.J.I., 2019. Slipped capital femoral epiphysis in an adult patient with kabuki syndrome. JAAOS Glob. Res. & Rev. 3 (10) e19.00084.
- Stewart, K.J., et al., 2004. Implementing capsule representation in a total hip dislocation finite element model. Iowa Orthop. J. 24, 1–8.
- Wako, M., et al., 2020. The characteristics of the whole pelvic morphology in slipped capital femoral epiphysis: a retrospective observational study. Medicine (Baltimore) 99 (14), e19600.
- Wiemann, J.M.I., Herrera-Soto, J.A., 2013. Can we Alter the natural history of osteoarthritis after SCFE with early realignment? J. Pediatr. Orthop. 33, S83–S87.
- Wu, G., et al., 2002. ISB recommendation on definitions of joint coordinate system of various joints for the reporting of human joint motion-part I: ankle, hip, and spine. International Society of Biomechanics. J. Biomech. 35 (4), 543–548.
- Yadav, P., Shefelbine, S.J., Gutierrez-Farewik, E.M., 2016. Effect of growth plate geometry and growth direction on prediction of proximal femoral morphology. J. Biomech. 49 (9), 1613–1619.
- Yoshimoto, H., et al., 2005. Spinopelvic alignment in patients with osteoarthrosis of the hip: a radiographic comparison to patients with low Back pain. Spine 30 (14), 1650–1657.
- Zupanc, O., et al., 2008. Shear stress in epiphyseal growth plate is a risk factor for slipped capital femoral epiphysis. J. Pediatr. Orthop. 28 (4), 444–451.